



Published in final edited form as:

Anesth Analg. 2008 September ; 107(3): 1045–1051. doi:10.1213/ane.0b013e31817bd1f0.

Restoration of Calcium Influx Corrects Membrane Hyperexcitability in Injured Rat Dorsal Root Ganglion Neurons

Quinn Hogan, M.D.^{a,h}, Philipp Lirk, M.D.^{b,e}, Mark Poroli, B.S.^c, Marcel Rigaud, M.D.^{b,f}, Andreas Fuchs, M.D.^{b,f}, Patrick Fillip, M.D.^d, Marko Ljubkovic, M.D.^{b,g}, and Damir Sapunar, M.D., Ph.D.^{b,g}

^aProfessor, Department of Anesthesiology, Medical College of Wisconsin, Milwaukee WI, USA

^bResearch Fellow, Department of Anesthesiology, Medical College of Wisconsin, Milwaukee WI, USA

^cResearch Technologist, Department of Anesthesiology, Medical College of Wisconsin, Milwaukee WI, USA

^dResident, Department of Anesthesiology, Medical College of Wisconsin, Milwaukee WI, USA

^eDepartment of Anesthesiology and Critical Care Medicine, Medical University of Innsbruck, Austria

^fDepartment of Intensive Care and Anesthesiology, Medical University of Graz, Austria

^gUniversity of Split Medical School, Split, Croatia

^hStaff Anesthesiologist, Milwaukee Veterans Administration Medical Center.

Abstract

We have previously shown that a decrease of inward Ca^{2+} flux (I_{Ca}) across the sensory neuron plasmalemma, such as happens after axotomy, elevates neuronal excitability. From this, we predicted that increasing I_{Ca} in injured neurons should correct their hyperexcitability, which we have tested during recording from A-type neurons in non-dissociated dorsal root ganglia after spinal nerve ligation, using an intracellular recording technique. When bath Ca^{2+} level was elevated to promote I_{Ca} , the afterhyperpolarization was decreased and repetitive firing was suppressed, which also followed amplification of Ca^{2+} -activated K^+ current with selective agents NS1619 and NS309. Lowered external bath Ca^{2+} concentration had opposite effects, similar to previous observations in uninjured neurons. These findings indicate that at least a part of the hyperexcitability of somatic sensory neurons after axotomy is attributable to diminished inward Ca^{2+} flux, and that measures to restore I_{Ca} may potentially be therapeutic for painful peripheral neuropathy.

Implications Statement: Restoring I_{Ca} in injured A-type sensory neurons leads to decreased neuronal excitability. Increasing inward Ca^{2+} flux may potentially be therapeutic for painful peripheral neuropathy.

Introduction

Various laboratories, including our own, have observed a decreased inward Ca^{2+} flux (I_{Ca}) in axotomized somatic sensory neurons (1–5), which are also noted to be hyperexcitable (6,7). We have recently shown that suppression of I_{Ca} in uninjured neurons produces changes that simulate axotomy, including a diminished duration and area of the afterhyperpolarization (AHP), a decreased current threshold for action potential (AP) initiation, and increased

repetitive firing during sustained depolarization [cite companion paper]. From these observations, we speculate that depressing I_{Ca} should have less effect on injured sensory neurons in which prior loss of I_{Ca} would preclude this action. More importantly, these findings also predict that increasing I_{Ca} in injured sensory neurons will correct their aberrant hyperexcitability, which would have translational importance. Accordingly, we have tested the effects of manipulating I_{Ca} in sensory neurons from animals made hyperalgesic by peripheral nerve injury. Since activation of Ca^{2+} -dependent K^+ current ($I_{K(Ca)}$) is a critical downstream mechanism through which I_{Ca} regulates neuronal excitability (8–11), we additionally tested the response of injured neurons to agents that selectively increase $I_{K(Ca)}$ through elevating the Ca^{2+} sensitivity of specific channel subtypes.

Materials and Methods

All procedures used in the study were approved by the Animal Resource Center of the Medical College of Wisconsin.

Animal Preparation

During isoflurane anesthesia (2% in oxygen), spinal nerve ligation (SNL) was performed on male Sprague-Dawley rats (200–300g) at the fifth lumbar (L5) and L6 levels with 6-0 silk ligature and distal transection, which was confirmed at the time of tissue harvest. Unlike the originally described method (12), paraspinal muscles and the adjacent articular process were not removed.

Behavioral Testing

Sensory responsiveness was tested using a method that we have validated for selective identification of neuropathic hyperalgesia (13). On 3 separate days in the second and third postoperative weeks, each hind surface was touched with a 22g spinal anesthesia needle with pressure adequate to indent the plantar skin. Tissue was harvested only from animals that displayed a hyperalgesia-type response with sustained paw lifting, shaking or licking (70% of the injured animals).

Tissue Preparation and Electrophysiological Recording

Methods are similar to those described previously [cite companion paper]. Briefly, ganglia were removed 20 ± 3 days after surgery, a time at which hyperalgesia has fully developed (13). During anesthesia, the L5 DRG and attached dorsal roots were removed. After removal of the capsule, the DRG was secured in a recording chamber and perfused with 35°C artificial CSF (aCSF, in mM: NaCl 128, KCl 3.5, MgCl_2 1.2, CaCl_2 2.3, NaH_2PO_4 1.2, NaHCO_3 24.0, glucose 11.0) aerated by 5% CO_2 and 95% O_2 to maintain a pH of 7.35. The dorsal roots were placed on stimulating electrodes for generation of conducted action potentials (APs). DRG somata were impaled with microelectrodes filled with 2_M potassium acetate (80–120 $\text{M}\Omega$) during microscopy using differential interference contrast optics and infrared illumination. Membrane potential was recorded using an active bridge amplifier (Axoclamp 2B, Axon Instruments, Foster City, CA), or discontinuous current clamp recording mode (2kHz switching) for recording voltage during current injection through the recording pipette. Data was digitized at 10kHz (discontinuous) or 20 kHz data acquisition and analysis (bridge; Digidata 1322A and Axograph 4.9, Axon Instruments).

APs measures (Fig. 1) included AP and AHP durations and the area under the curve for the AHP (AHParea), and slope of the ascending limb (dV/dt) determined from the differentiated trace. Input resistance was calculated from the hyperpolarization during 100ms current injection (0.5nA) (14). Voltage “sag” in response to hyperpolarization, attributable to the H-current (15), was quantified as the fractional return from the peak hyperpolarization during

100ms of 1.2nA hyperpolarization current injection. Rheobase was determined as the minimum current able to elicit an AP during incremental injection of depolarizing current (0.5–10nA for 100ms) directly to the soma through the recording electrode. The pattern of impulse generation was determined during depolarizing current steps beyond rheobase, at which neurons either continued to produce single APs or fired repetitively. The influence of bath Ca^{2+} level or drug upon AP firing pattern was measured at a depolarizing voltage that first produced a bath Ca^{2+} - or drug-induced difference in the number of APs generated.

Neurons were classified by conduction velocity (CV) calculated from conducted distance and latency. Adequately stable C-type neuron ($\text{CV} < 1.5\text{m/S}$) recordings were too few to report. Neurons with $\text{CV} > 15\text{m/S}$ were considered $\text{A}\alpha/\beta$ -type, and neurons with $\text{CV} > 1.5\text{m/S}$ but $\text{CV} < 10\text{m/S}$ were considered $\text{A}\delta$ -type. For neurons with CV between 10 and 15m/S, long AP duration was used to categorize the cells as $\text{A}\delta$ -types (14).

Ca^{2+} current modulation

To test whether injury precludes responses to lowered I_{Ca} , we examined effects of lowering bath Ca^{2+} on L5 neurons after SNL ($n = 14 \text{ A}\alpha/\beta$ and 12 $\text{A}\delta$). After baseline electrophysiologic parameters were measured in aCSF, ganglia were exposed by bath change to an identical external solution except for a lower Ca^{2+} concentration achieved by substituting CaCl_2 with MgCl_2 , producing a measured Ca^{2+} concentration of 0.35 mM. This reduces I_{Ca} by to only 6% of baseline [cite companion paper]. Magnesium was added to a final concentration of 3.5mM in order to exclude the possible influence of changed surface charge (16), and to maintain a constant divalent cation effect on potassium channels (17). To test whether augmenting I_{Ca} reverses the effects of injury, SNL L5 neurons ($n = 24 \text{ A}\alpha/\beta$ and 21 $\text{A}\delta$) were exposed to a bath Ca^{2+} level of 7mM. This solution elevates I_{Ca} by 35% [cite companion paper]. Effects were measured after a wash-in interval of 3 min.

To explore the mechanism of the action of increasing I_{Ca} , we sought out repetitively firing neurons to expose to the $\text{I}_{\text{K}(\text{Ca})}$ activators NS1619 ($10\mu\text{M}$), which selectively increases current through the large conductance (BK) channel (18,19), or NS309 ($5\mu\text{M}$), which increases current through the small conductance (SK) and intermediate conductance (IK) channel subtypes (20,21). These were delivered by a microperfusion technique from a pipette with a $10\mu\text{m}$ diameter tip that was positioned 200μ from the impaled neuron, and ejected continuously by pressure applied to the back end of the pipette (Picospritzer II, General Valve Corp, Fairfield, NJ). Preliminary experiments indicated an effective 5-fold dilution of pipette solution into the bath at the cell surface, so pipette concentrations of $50\mu\text{M}$ for NS1619 and $25\mu\text{M}$ NS309 were used.

All agents were purchased from Sigma-Aldrich Co. (St. Louis, MO).

Data Analysis and Statistics

Data are expressed as means \pm SD. The effect of bath changes was evaluated using paired Student's *t*-test to identify of significant drug effects in the context of natural variability between neurons under baseline conditions. Significance was accepted at $P < 0.05$.

Results

Effects of injury

SNL rats from which tissue was harvested showed a greater frequency of hyperalgesia-type responses ipsilateral to the injury ($34 \pm 6\%$; $n = 37$) than a contemporaneous control group of animals that had only a midline lumbar skin incision and staple closure ($1 \pm 1\%$; $n = 68$, $P < 0.001$).

Although this study was not designed to determine the effects of injury on electrophysiological parameters, we note that, in comparison to a previously reported control group that was studied concurrently with the experiments reported here [cite companion paper], axotomized L5 neurons after SNL developed electrophysiological changes consistent with those shown in previous examination of the effects of injury (6), including decreased AP amplitude and upstroke velocity, increased AP duration, and decreased AHP.

Decreasing I_{Ca} in injured neurons

We predicted that the injury-related loss of I_{Ca} should preclude effects of further decreasing I_{Ca} by bath Ca^{2+} withdrawal in axotomized neurons. In fact (Table 1), low bath Ca^{2+} produced significant decreases in AHP dimensions and in rheobase that resembled changes seen in uninjured neurons [cite companion paper] and exceeded them in magnitude. Lowering bath Ca^{2+} also decreased AP amplitude in axotomized $A\alpha/\beta$ neurons, but not in $A\delta$ neurons, and inflection disappeared in 3 of 8 neurons, which is also similar to the effect observed in control neurons. A tendency for increased firing during depolarization was demonstrated, as 5 neurons showed increased firing, 18 were unchanged, and 1 fired less. Unlike control neurons, axotomized neurons showed no decrement in hyperpolarization-induced voltage sag during Ca^{2+} withdrawal in both $A\alpha/\beta$ and $A\delta$ neurons.

Increasing I_{Ca} in injured neurons

We next tested the hypothesis that certain aspects of abnormal membrane behavior of axotomized neurons might be repaired by increased I_{Ca} . During elevation of bath Ca^{2+} (Table 1; Fig. 2), $A\alpha/\beta$ and $A\delta$ neurons from the fifth lumbar DRG following SNL developed increased AHP amplitude, AHP area, and rheobase, reversing the effects produced by injury (6). Also, the number of APs during sustained depolarization decreased in all repetitively firing injured neurons during high bath Ca^{2+} . Specifically, the average number of APs in repetitively firing $A\alpha/\beta$ neurons decreased from 4.1 ± 0.8 to 2.0 ± 0.5 ($P < 0.01$, $n = 10$), and the number of APs in repetitively firing $A\delta$ neurons decreased from 3.0 ± 0.9 to 2.1 ± 0.8 ($P < 0.05$, $n = 10$), indicating the stabilization of these injured neurons by increased I_{Ca} (Fig. 3). All of the accommodating, single firing neurons (12 $A\alpha/\beta$, 8 $A\delta$) remained so during the elevation of bath Ca^{2+} . In both $A\alpha/\beta$ and $A\delta$ injured neurons, increasing I_{Ca} with elevated bath Ca^{2+} concentration slowed the conduction velocity. This demonstrates that the decrease in conduction velocity caused by injury cannot be attributed to injury-induced loss of I_{Ca} , but instead is probably due to a shift in the balance of various sodium current subtypes (22).

Increasing $I_{K(Ca)}$ in injured neurons

Both $I_{K(Ca)}$ enhancers NS309 and NS1619 produced effects that resembled exposure to high bath Ca^{2+} and reversed changes that follow injury (Table 2). Specifically, stimulation of SK and IK-type Ca^{2+} -activated K^+ channels with NS309 increased the rheobase, expanded the AHP, and caused all 7 repetitively firing neurons (4 $A\alpha/\beta$, 3 $A\delta$) to fire less during depolarization (3.29 ± 1.60 APs at baseline, 1.14 ± 0.38 APs during NS309, $P < 0.01$; Fig. 4). Stimulation of BK-type Ca^{2+} -activated K^+ current with NS1619 also increased the rheobase, but did not increase AHP dimensions, consistent with its action on the earliest part of the repolarization phase (11). Like exposure to high bath Ca^{2+} , NS1619 decreased the number of APs during neuron depolarization in all 8 repetitively firing neurons (6 $A\alpha/\beta$, 2 $A\delta$; 3.50 ± 2.10 APs at baseline, 1.63 ± 0.92 APs during NS1619, $P < 0.01$).

Discussion

Our results show that elevation of extracellular Ca^{2+} , which increases I_{Ca} , reverses the loss of AHP and elevated excitability of sensory neurons that follows peripheral nerve trauma. We, as well as others, have previously demonstrated a loss of I_{Ca} in axotomized primary sensory

neurons, so the present observations support a role for this I_{Ca} loss in generating post-traumatic hyperexcitability.

In contrast with our expectations, axotomized L5 neurons after SNL still respond to depression of I_{Ca} with elevated indices of excitability, including a decreased current necessary for AP initiation (rheobase), decreased AHP dimensions, and an associated increased propensity for repetitive firing. This may be explained by a heightened sensitivity to further loss of I_{Ca} due to the already deficient I_{Ca} due to injury. This is supported by a prior study of dissociated sensory neurons in which hyperexcitability developed in axotomized neurons when intracellular Ca^{2+} levels were buffered at a low level, while this did not occur with control neurons (23).

Calcium that enters through neuronal plasmalemmal Ca^{2+} channels has numerous regulatory functions, including the modulation of firing patterns by activation of $I_{K(Ca)}$ and generation of the AHP. We previously demonstrated expression of $I_{K(Ca)}$ currents sensitive to blockers of BK, IK, and SK types of $I_{K(Ca)}$ rat DRG neurons (24). In the present experiments, we tested the role $I_{K(Ca)}$ as a downstream effector by which increased inward Ca^{2+} flux may depress excitability, using agents that directly enhance current through these channels. The results were similar to elevating I_{Ca} , including enhanced AHP and diminished repetitive firing. Also, similar to increased I_{Ca} during elevated bath Ca^{2+} , enhanced $I_{K(Ca)}$ increased rheobase, which indicates a depressed neuronal tendency to trigger an initial AP. This effect is possibly due to the enhanced $I_{K(Ca)}$ competing with the inward depolarizing currents during the nascent initial phase of AP generation (Fig. 4).

Our previous observations indicate that axotomy is associated with both diminished I_{Ca} (1–3) and a loss of recruitable Ca^{2+} -activated K^+ channels (24) in sensory neurons. Our findings in the present study indicate that neuronal function after injury may be returned towards normal by elevating I_{Ca} , which may act through amplification of $I_{K(Ca)}$. These findings imply that measures designed increase inward Ca^{2+} flux in sensory neurons may provide analgesia following peripheral nerve trauma. Enhanced function of Ca^{2+} channels through rapidly advancing molecular technology may be one path to achieve this goal.

Acknowledgments

Supported by grant NS-42150 from the National Institutes of Health, Bethesda, Maryland, USA to QH.

References

1. McCallum JB, Kwok WM, Mynlieff M, et al. Loss of T-type calcium current in sensory neurons of rats with neuropathic pain. *Anesthesiology* 2003;98:209–216. [PubMed: 12502999]
2. McCallum JB, Jednacak K, Seagard JL, Hogan QH. Loss of I_{Ca} in sensory neurons after spinal nerve ligation and sham surgery. *Society for Neuroscience Abstracts*. 2002
3. Hogan QH, McCallum JB, Sarantopoulos C, et al. Painful neuropathy decreases membrane calcium current in mammalian primary afferent neurons. *Pain* 2000;86:43–53. [PubMed: 10779659]
4. Baccei ML, Kocsis JD. Voltage-gated calcium currents in axotomized adult rat cutaneous afferent neurons. *Journal of Neurophysiology* 2000;83:2227–2238. [PubMed: 10758131]
5. Abdulla FA, Smith PA. Axotomy- and autotomy-induced changes in Ca^{2+} and K^+ channel currents of rat dorsal root ganglion neurons. *Journal of Neurophysiology* 2001;85:644–658. [PubMed: 11160500]
6. Sapunar D, Ljubkovic M, Lirk P, et al. Distinct membrane effects of spinal nerve ligation on injured and adjacent dorsal root ganglion neurons in rats. *Anesthesiology* 2005;103:360–376. [PubMed: 16052119]
7. Abdulla FA, Smith PA. Axotomy- and autotomy-induced changes in the excitability of rat dorsal root ganglion neurons. *Journal of Neurophysiology* 2001;85:630–643. [PubMed: 11160499]

8. Bahia PK, Suzuki R, Benton DC, et al. A functional role for small-conductance calcium-activated potassium channels in sensory pathways including nociceptive processes. *J Neurosci* 2005;25:3489–3498. [PubMed: 15814779]
9. Amir R, Devor M. Spike-evoked suppression and burst patterning in dorsal root ganglion neurons of the rat. *Journal of Physiology* 1997;501:183–196. [PubMed: 9175002]
10. Viana F, Bayliss DA, Berger AJ. Multiple potassium conductances and their role in action potential repolarization and repetitive firing behavior of neonatal rat hypoglossal motoneurons. *Journal of Neurophysiology* 1993;69:2150–2163. [PubMed: 8350136]
11. Scholz A, Gruss M, Vogel W. Properties and functions of calcium-activated K⁺ channels in small neurones of rat dorsal root ganglion studied in a thin slice preparation. *Journal of Physiology* 1998;513:55–69. [PubMed: 9782159]
12. Kim SH, Chung JM. An experimental model for peripheral neuropathy produced by segmental spinal nerve ligation in the rat. *Pain* 1992;50:355–363. [PubMed: 1333581]
13. Hogan Q, Sapunar D, Modric-Jednacak K, McCallum JB. Detection of neuropathic pain in a rat model of peripheral nerve injury. *Anesthesiology* 2004;101:476–487. [PubMed: 15277932]
14. Villiere V, McLachlan EM. Electrophysiological properties of neurons in intact rat dorsal root ganglia classified by conduction velocity and action potential duration. *Journal of Neurophysiology* 1996;76:1924–1941. [PubMed: 8890304]
15. Scroggs RS, Todorovic SM, Anderson EG, Fox AP. Variation in IH, IIR, and ILEAK between acutely isolated adult rat dorsal root ganglion neurons of different size. *Journal of Neurophysiology* 1994;71:271–279. [PubMed: 7512627]
16. Hille, B. *Ion Channels of Excitable Membranes*. Vol. 3rd ed.. Sunderland, MA, USA: Sinauer Associates; 2001.
17. Mayer ML, Sugiyama K. A modulatory action of divalent cations on transient outward current in cultured rat sensory neurones. *Journal of Physiology* 1988;396:417–433. [PubMed: 2457691]
18. Olesen SP, Munch E, Moldt P, Drejer J. Selective activation of Ca²⁺-dependent K⁺ channels by novel benzimidazolone. *Eur J Pharmacol* 1994;251:53–59. [PubMed: 8137869]
19. Zhang XF, Gopalakrishnan M, Shieh CC. Modulation of action potential firing by iberiotoxin and NS1619 in rat dorsal root ganglion neurons. *Neuroscience* 2003;122:1003–1011. [PubMed: 14643767]
20. Pedarzani P, McCutcheon JE, Rogge G, et al. Specific enhancement of SK channel activity selectively potentiates the afterhyperpolarizing current I(AHP) and modulates the firing properties of hippocampal pyramidal neurons. *J Biol Chem* 2005;280:41404–41411. [PubMed: 16239218]
21. Strobaek D, Teuber L, Jorgensen TD, et al. Activation of human IK and SK Ca²⁺-activated K⁺ channels by NS309 (6,7-dichloro-1H-indole-2,3-dione 3-oxime). *Biochim Biophys Acta* 2004;1665:1–5. [PubMed: 15471565]
22. Waxman SG, Dib-Hajj S, Cummins TR, Black JA. Sodium channels and pain. *Proceedings of the National Academy of Sciences of the United States of America* 1999;96:7635–7639. [PubMed: 10393872]
23. Hilaire C, Inquimbert P, Al-Jumaily M, et al. Calcium dependence of axotomized sensory neurons excitability. *Neurosci Lett* 2005;380:330–334. [PubMed: 15862912]
24. Sarantopoulos CD, McCallum JB, Rigaud M, et al. Opposing effects of spinal nerve ligation on calcium-activated potassium currents in axotomized and adjacent mammalian primary afferent neurons. *Brain Res* 2007;1132:84–99. [PubMed: 17184741]

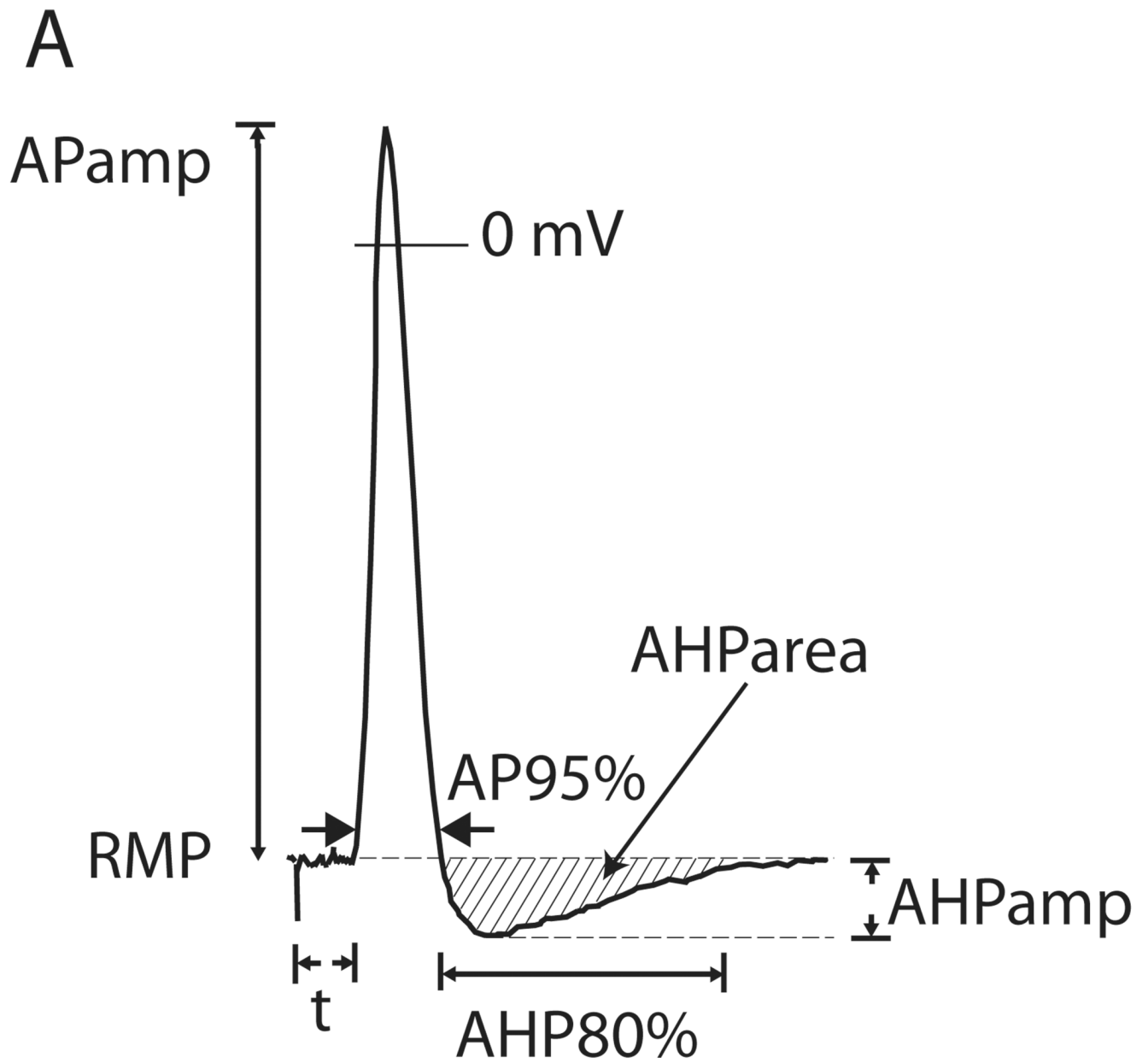


Figure 1. Measurements determined from action potential (AP) trace. RMP, resting membrane potential; APamp., amplitude of AP; AP95%, duration of AP at 95% of amplitude; t, latency following axonal stimulation; AHPamp., amplitude of afterhyperpolarization; AHP80%, duration of afterhyperpolarization until 80% recovery to baseline.

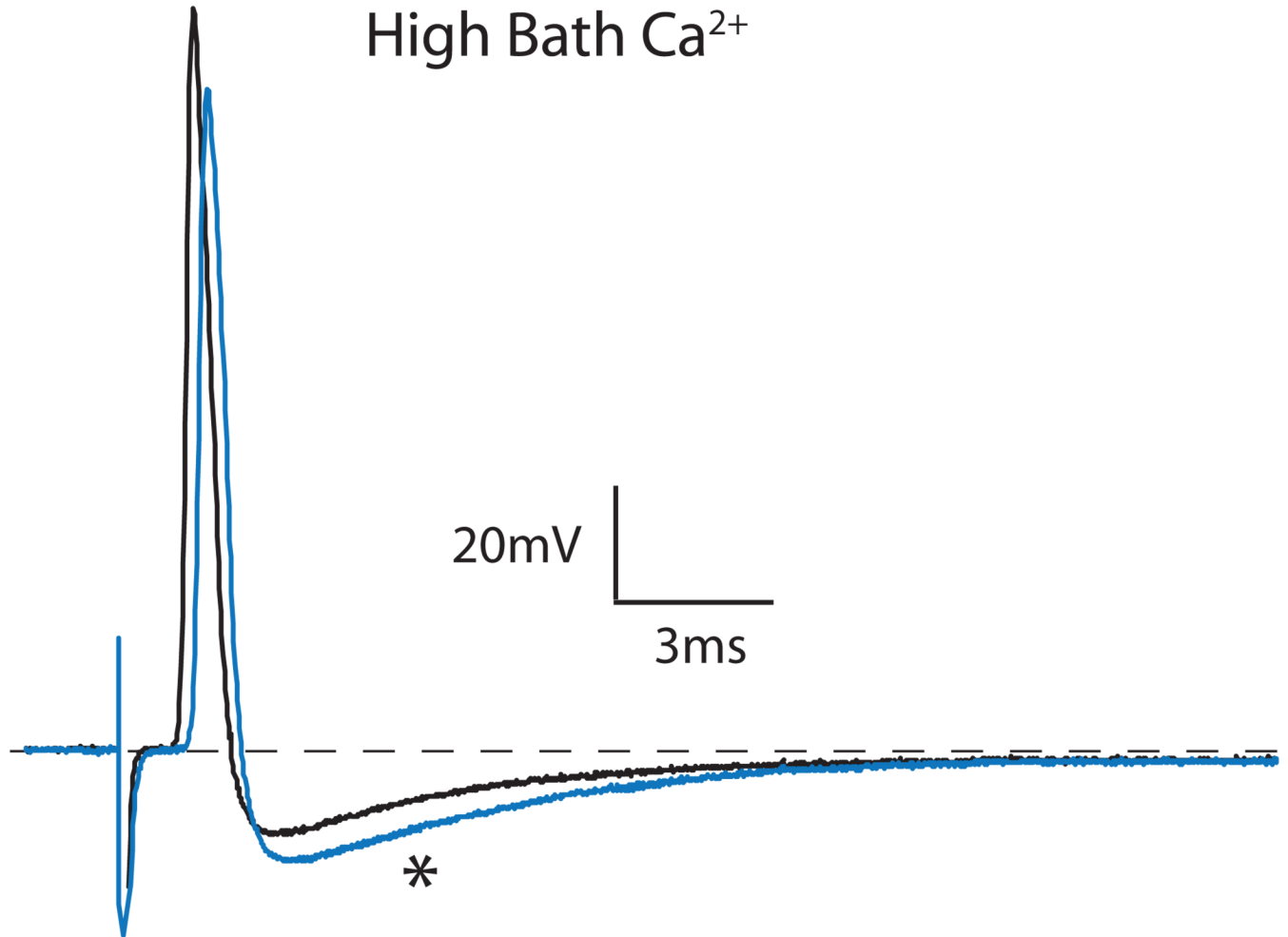


Figure 2. Influence of elevating bath Ca^{2+} concentration on an axotomized $\text{A}\alpha/\beta$ neuron. Elevation of bath Ca^{2+} concentration from 2.3 mM to 7 mM increased the amplitude and area of the afterhyperpolarization (*, blue trace).

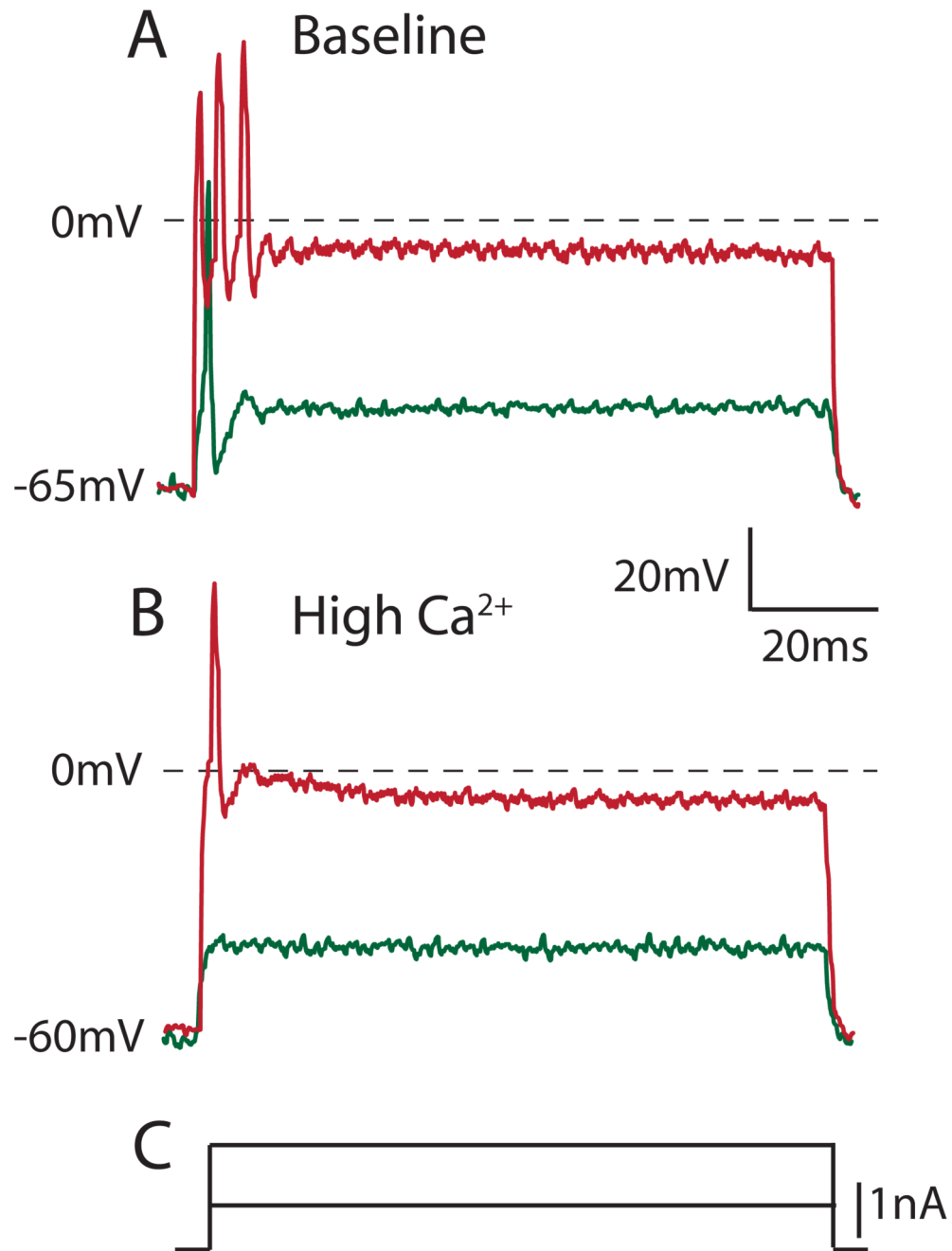


Figure 3. Increased bath Ca^{2+} concentration diminishes repetitive firing during depolarization of an axotomized $\text{A}\alpha/\beta$ sensory neuron. *A.* Under baseline conditions of 2.3 mM bath Ca^{2+} concentration, depolarizing current injection produces an initial single action potential, and further depolarization results in repetitive firing. *B.* Under high bath Ca^{2+} conditions (7 mM), current injection results initially in no action potential and subsequently only a single action potential using comparable depolarization steps (*C.*) as in *A.*

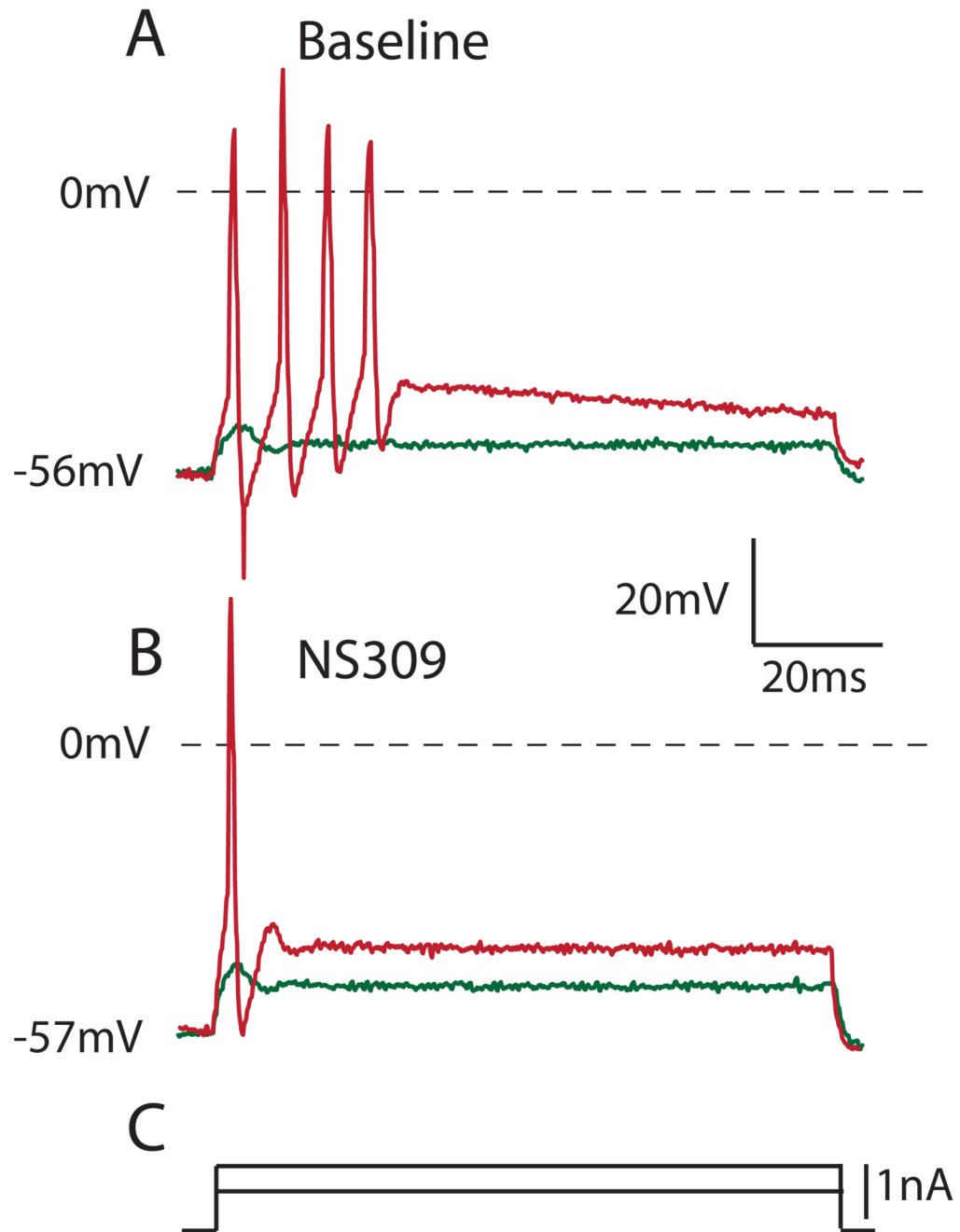


Figure 4. NS309 ($10\mu\text{M}$), which enhances Ca^{2+} -activated K^+ currents, reduces excitability in an axotomized $\text{A}\alpha/\beta$ sensory neuron (different from the neuron in Figure 3), similar to the action of high bath Ca^{2+} . *A.* Under baseline conditions, depolarizing current injection produces repetitive firing (red trace). *B.* During application of NS309, current injection results in only a single action potential (red) during comparable depolarization steps (*C.*) as in *A.* In both panels, a subthreshold current injection step induces an abortive depolarization that fails to produce a full action potential (green trace).

bath Ca²⁺ manipulation on active and passive membrane parameters on axotomized sensory neurons.

Table 1

RMP (mV)	CV (m/S)	APamp (mV)	AP95% (mS)	AHPamp (mV)	AHP80% (mS)	AHParea (mV·mS)	dV/dt (V/S)	R _{in} (MΩ)	Sag ratio (%)	Rheobase (nA)
-65.3±8.1	17.3±4.4	64.0±6.7	1.15±0.35	9.1±3.5	13.2±9.7	89.0±62.3	297±110	62.5±38.6	15.4±12.0	2.3±1.5
-65.8±9.1	17.9±4.4*	59.3±13.0	1.20±0.65	8.0±3.7*	7.9±7.1**	53.6±44.9**	261±115	52.6±28.5	15.8±14.3	1.8±1.2***
-66.7±10.7	8.4±2.3	73.3±16.2	1.76±0.48	9.5±3.1	29.0±34.0	196.2±174.8	279±139	89.4±66.8	11.6±6.9	2.4±1.0
-69.8±10.7	8.7±2.2*	72.9±13.1	1.65±0.65	8.8±4.2	9.5±3.5*	78.4±38.7**	259±112	118.5±107.5	11.2±9.3	1.3±0.7**
-69.7±7.7	18.2±6.6	73.1±9.8	1.25±0.61	8.8±3.2	18.4±20.9	141.0±146.0	351±133	63.9±55.6	21.9±15.6	1.4±0.7
-69.1±7.9	15.4±5.6***	69.0±10.7***	1.23±0.54	10.5±3.3***	17.2±18.2	168.2±167.4*	326±162*	76.0±87.2	20.6±13.2	1.8±1.0***
-71.0±9.5	8.2±3.1	74.4±16.6	2.04±1.17	8.7±4.1	24.9±22.5	145±150	254±107	133.1±121.8	11.9±11.8	1.1±0.7
-66.7±9.2**	8.2±2.5**	74.1±15.2	1.95±1.32	10.8±5.0***	26.8±30.4	199±198**	232±87*	105.5±95.2	10.1±10.9	1.4±0.9**

Baseline condition; RMP, resting membrane potential; CV, conduction velocity; APamp action potential amplitude; AP95% action potential duration at 95% of amplitude; AHP80% afterhyperpolarization duration at 80% of amplitude; AHParea afterhyperpolarization area under the curve; dV/dt maximum action potential upstroke

Table 2

Effects of Ca²⁺-activated K⁺ current enhancers NS309 and NS1619 on function of injured dorsal root ganglion neurons.

Agent	RMP (mV)	CV (m/s)	APamp (mV)	AP95% (ms)	AHPamp (mV)	AHP80% (ms)	AHParea (mV·ms)	R _{in} (MΩ)	Sag ratio (%)	Rheobase (nA)
vβ =11	BL	21.0±3.2	58.6±9.8	1.67±0.36	8.5±3.9	36 ±46	210±227	114±25	18.30±9.3	1.4±0.8
	NS309	20.9±3.9	58.9±10.1	1.65±0.36	8.9±3.5	213±261*	2007±2373*	115±29	18.9±10.6	1.6±0.9**
δ =8	BL	9.4±3.0	64.4±6.6	2.02±0.77	11.1±3.3	127±162	1321±912	90.3±36.3	16.0±11.5	2.2±1.3
	NS309	9.5±3.0	63.2±7.0	1.80±0.48	11.7±2.9	406±260**	2800±1020**	99.1±47.3	19.3±9.0	2.5±1.4**
vβ =7	BL	20.7±7.6	78.1 ±7.3	1.45±0.31	11.1±1.7	14.1±9.4	130±75	68.2±32.9	33.1±12.1	0.6±0.3
	NS1619	20.4±7.9	76.7±10.4	1.50±0.31**	10.1±2.0*	12.5±7.7	110±67*	62.6±33.5**	32.1±14.4	0.9±0.4**
δ =7	BL	9.9±3.2	79.8±13.0	2.06±0.63	11.7±3.4	27.6±25.5	403±291	85.6±40.2	19.0±19.1	1.3±1.1
	NS1619	9.7±3.2*	79.9±15.1	1.97±0.51	12.1±3.8	20.6±17.7*	346±253*	99.8±44.6	19.6±17.8	1.9±1.0***

Values are given as mean ± SD. BL Baseline condition; RMP resting membrane potential; CV conduction velocity; APamp action potential amplitude; AP95% action potential duration at 95% of amplitude; AHPamp afterhyperpolarization duration at 80% of amplitude; AHP80% afterhyperpolarization area under the curve; R_{in} input resistance.

*0.05

**<0.01

***P <0.001 vs. baseline.